

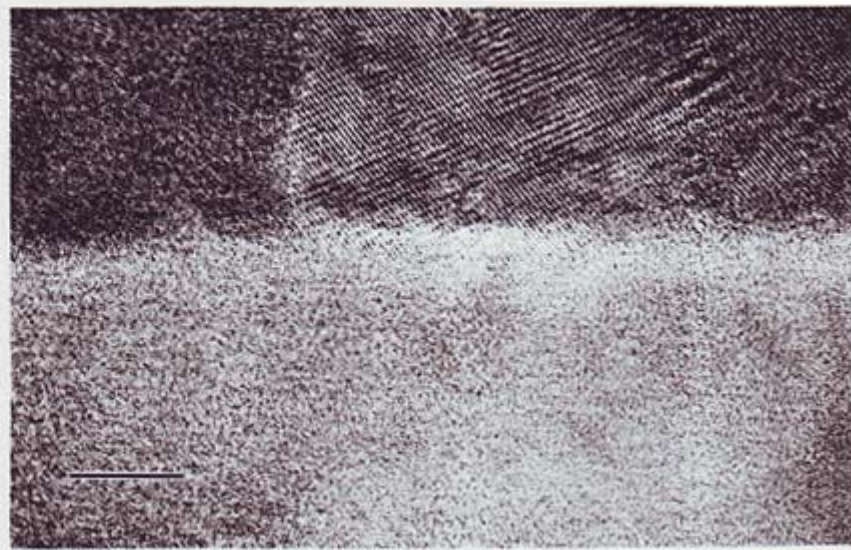
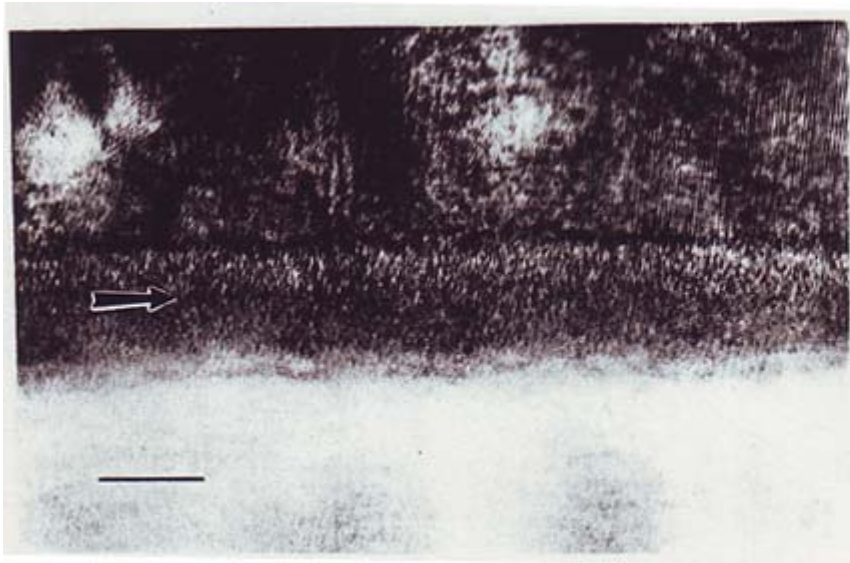
Thermochemical Effects at Multicomponent Glass Surfaces

Carlo G Pantano
Department of Materials Science and Engineering
Materials Research Institute
The Pennsylvania State University

Acknowledgements: Bob Hengstebeck
Justin Wood
CQ Shen
Elam Leed
Rob Schaut
Prof Karl Mueller
NSF Center for Glass Research

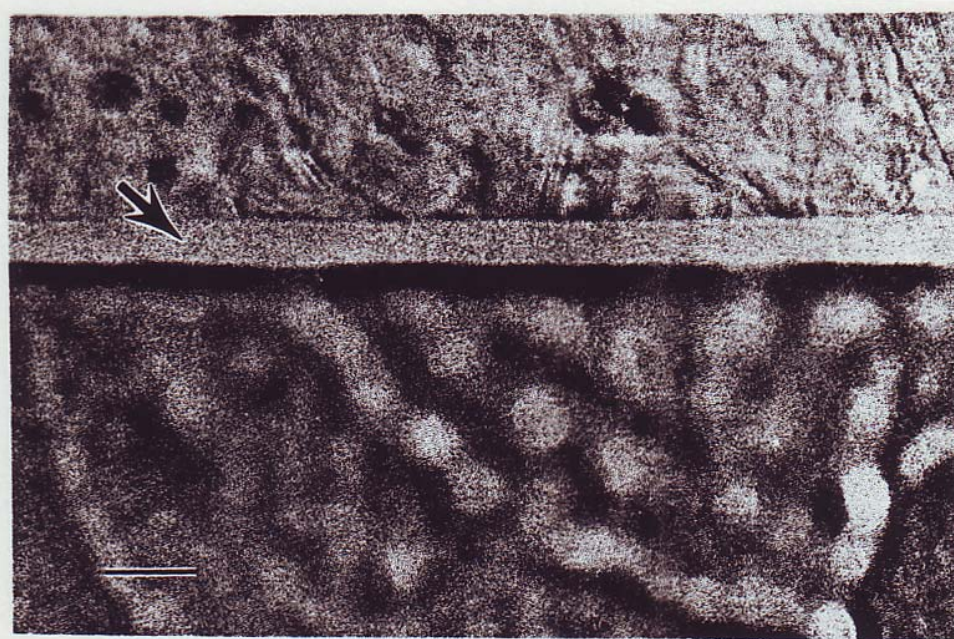
outline

- surface composition changes during fiberglass processing
- surface segregation during the fabrication of micro-sheet for display glass
- composition \leftrightarrow structure effects at surfaces.... BORON-OXIDE
- surface atomic structure models and their validation by adsorption



crystallized amorphous
silicon on various
glass substrates....

note interphases

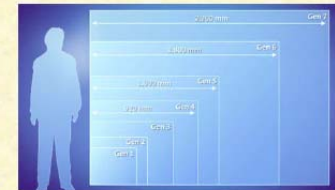


some opportunities for glass surface modification

- controlled electrical conductivity
- ‘primed’ for adhesion
- ‘hardened’ for abrasion resistance
- anti-reflective or highly reflective
- soluble or insoluble

Commercial Glass Dielectrics

- Large scale processes have been developed for producing thin glass sheets.
- Commercial market is growing rapidly for flat panel displays.
- Companies are interested in exploring new markets for flat panel glass.



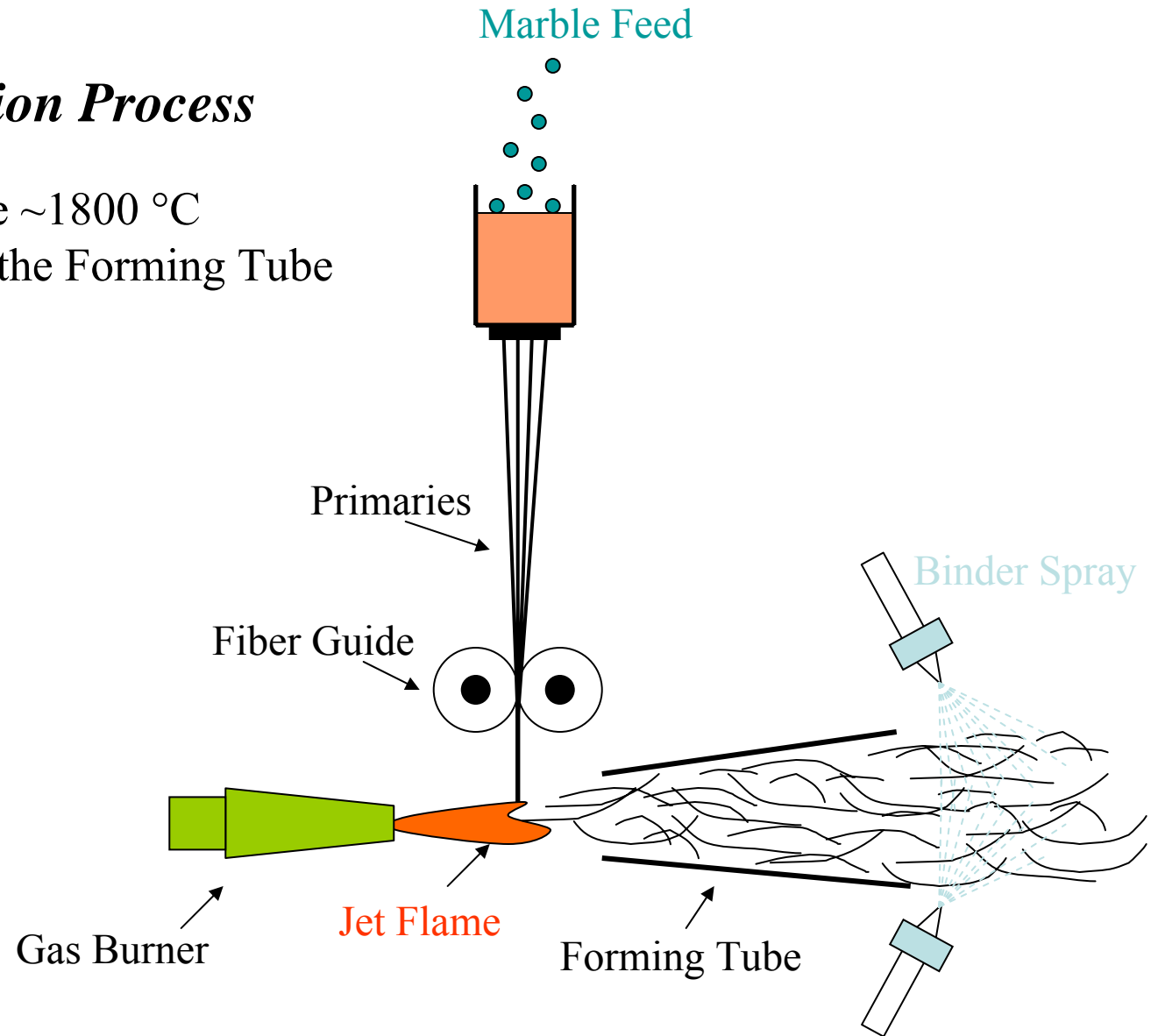
Projected glass plate dimensions for active matrix liquid crystal displays. The glass may be an excellent commodity material for high temperature capacitors for use in hybrid electric vehicles.

the 'surfaces' of most functional glasses come into existence in a temperature range where surface energy can be minimized through composition and/or structure changes, where evaporation of volatile species occurs, and where local redox equilibria can be established through adsorption and/or ion transport

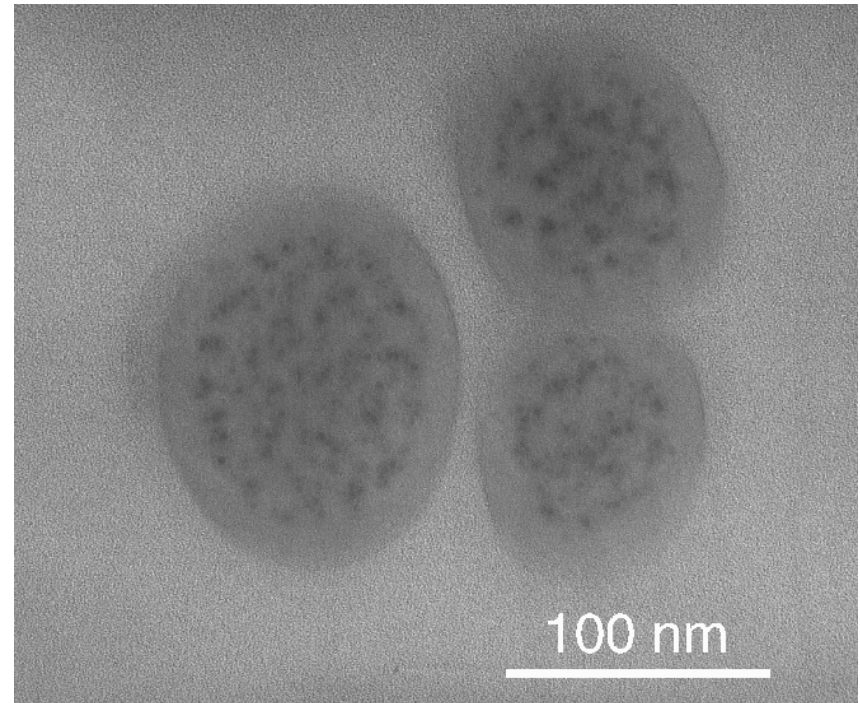
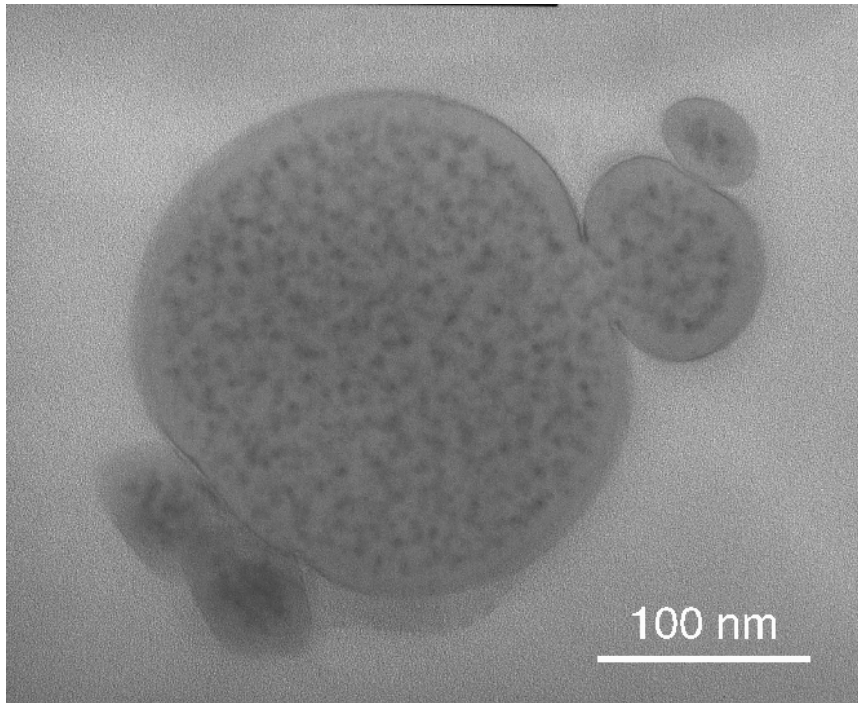
- thermal segregation
- changes in local coordination.. B_2O_3
- alkali, alkali borate, etc evaporation
- cation out-diffusion usually faster than O_2 in-diffusion
- redox equilibria drives cation oxidation on cooling

Flame Attenuation Process

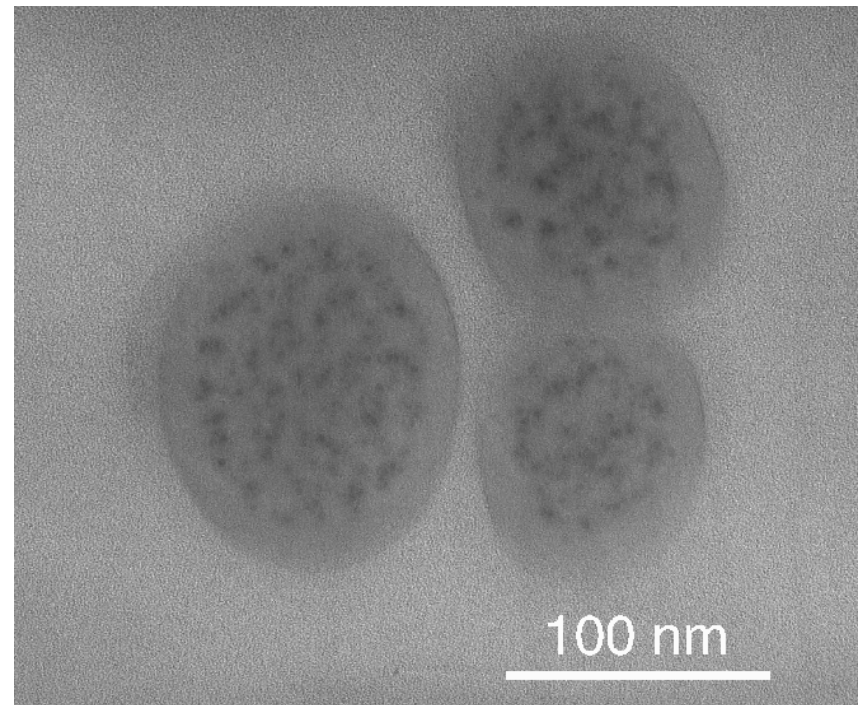
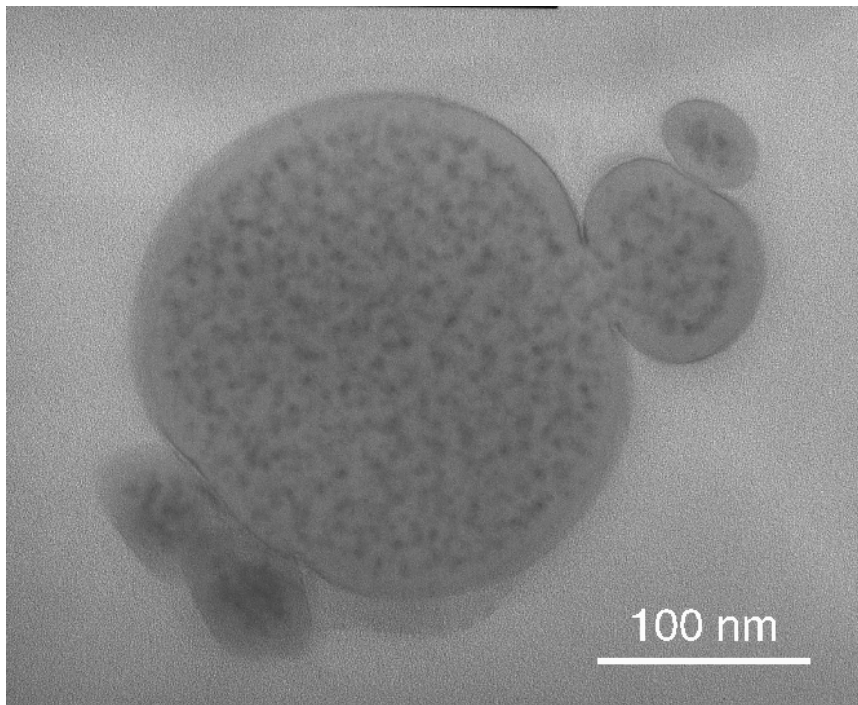
Flame Temperature $\sim 1800\text{ }^{\circ}\text{C}$
Slower Cooling in the Forming Tube



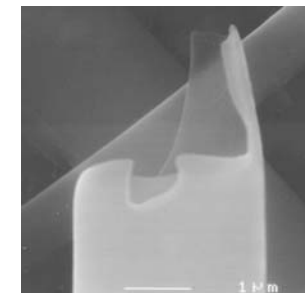
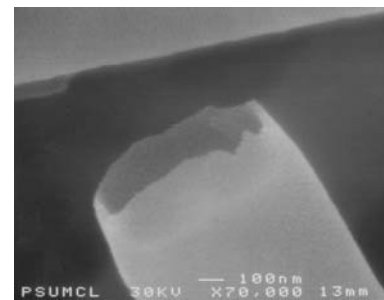
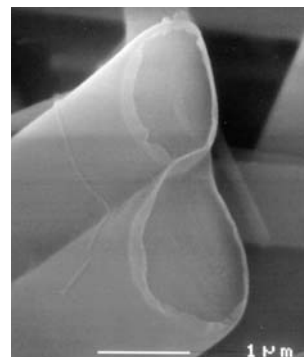
TEM of FA Nano Fibers



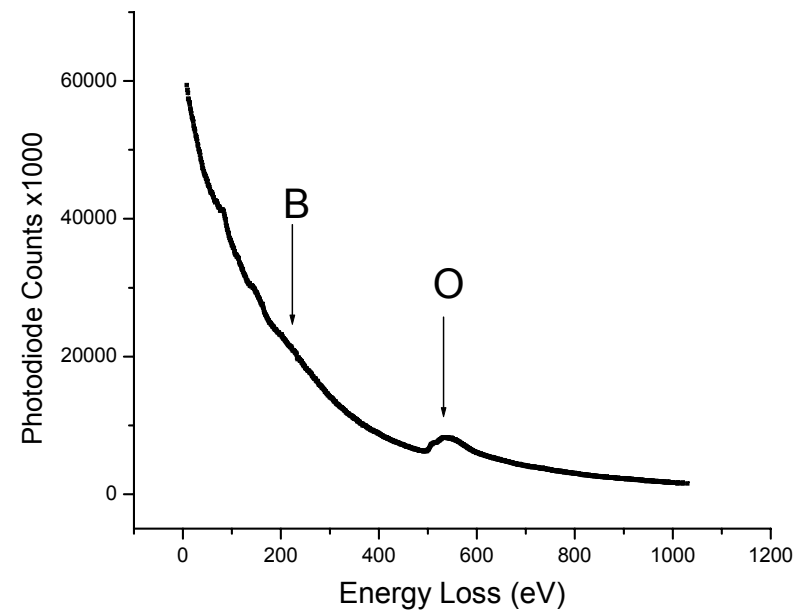
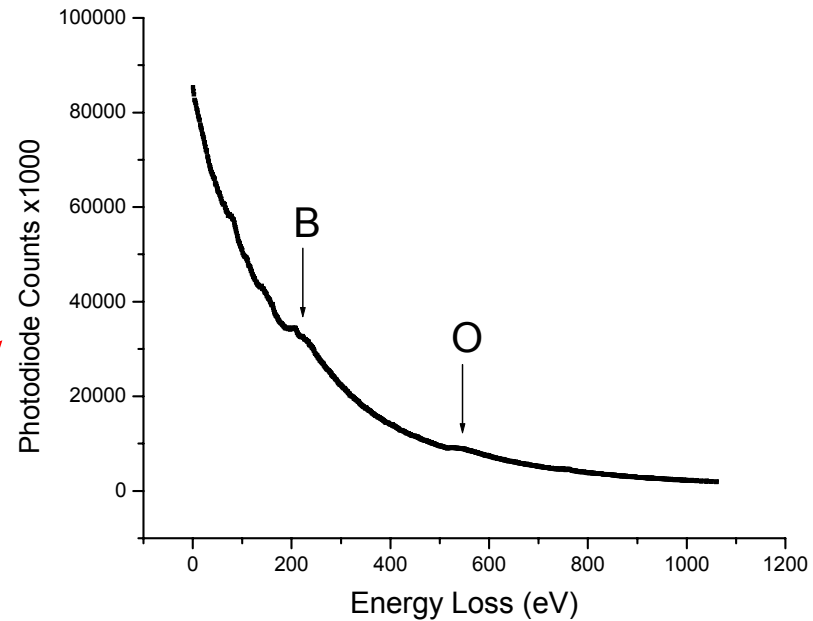
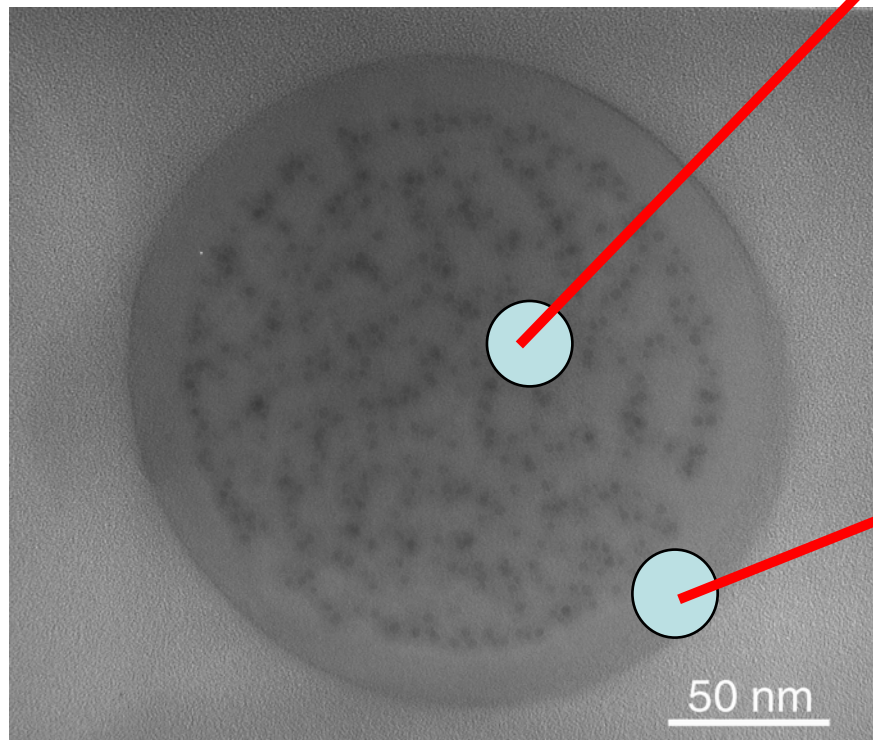
TEM of FA Fibers (Glass A)



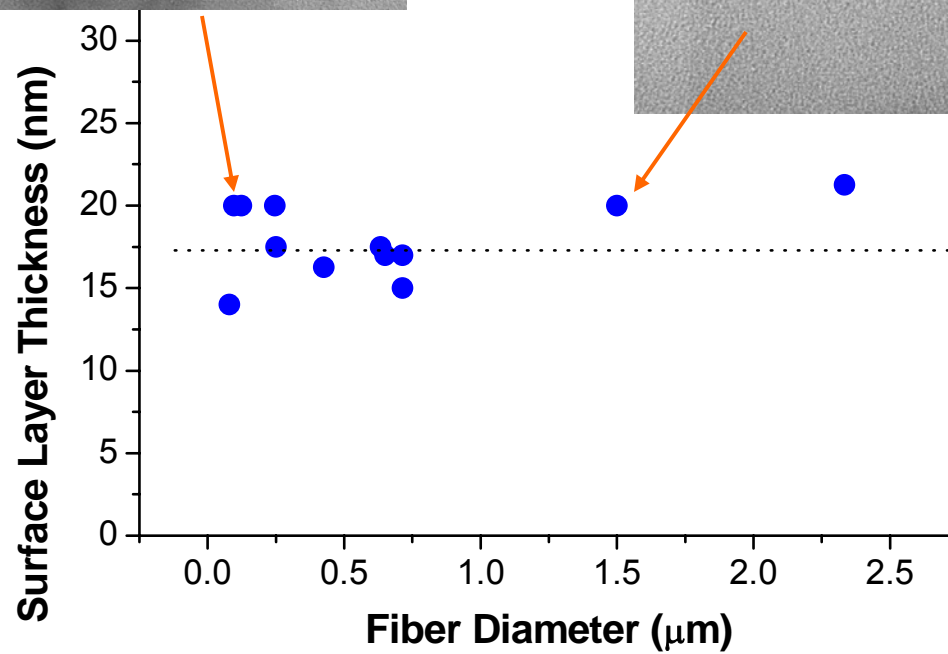
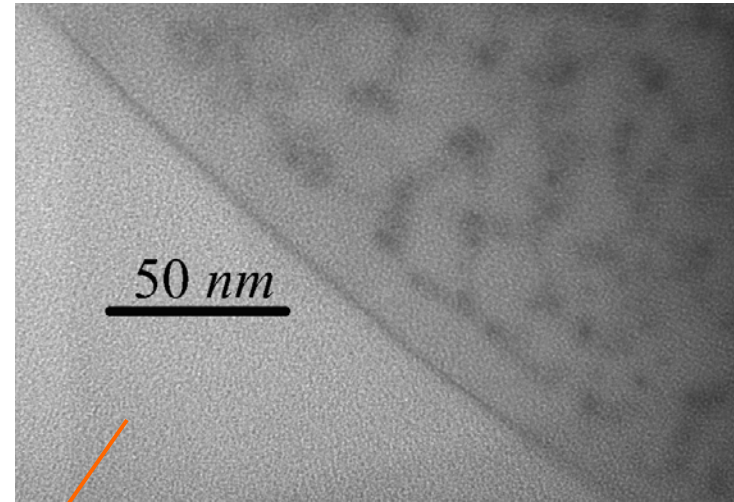
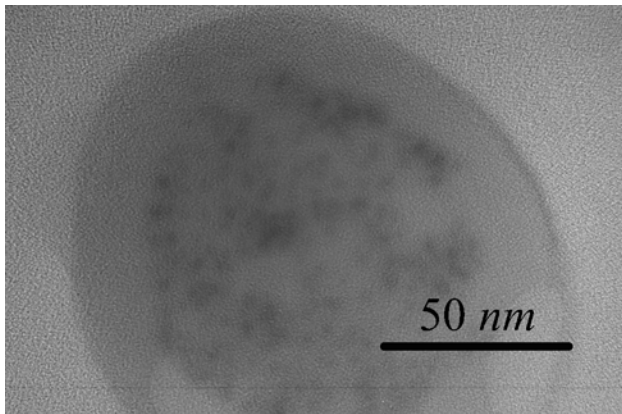
after leaching →



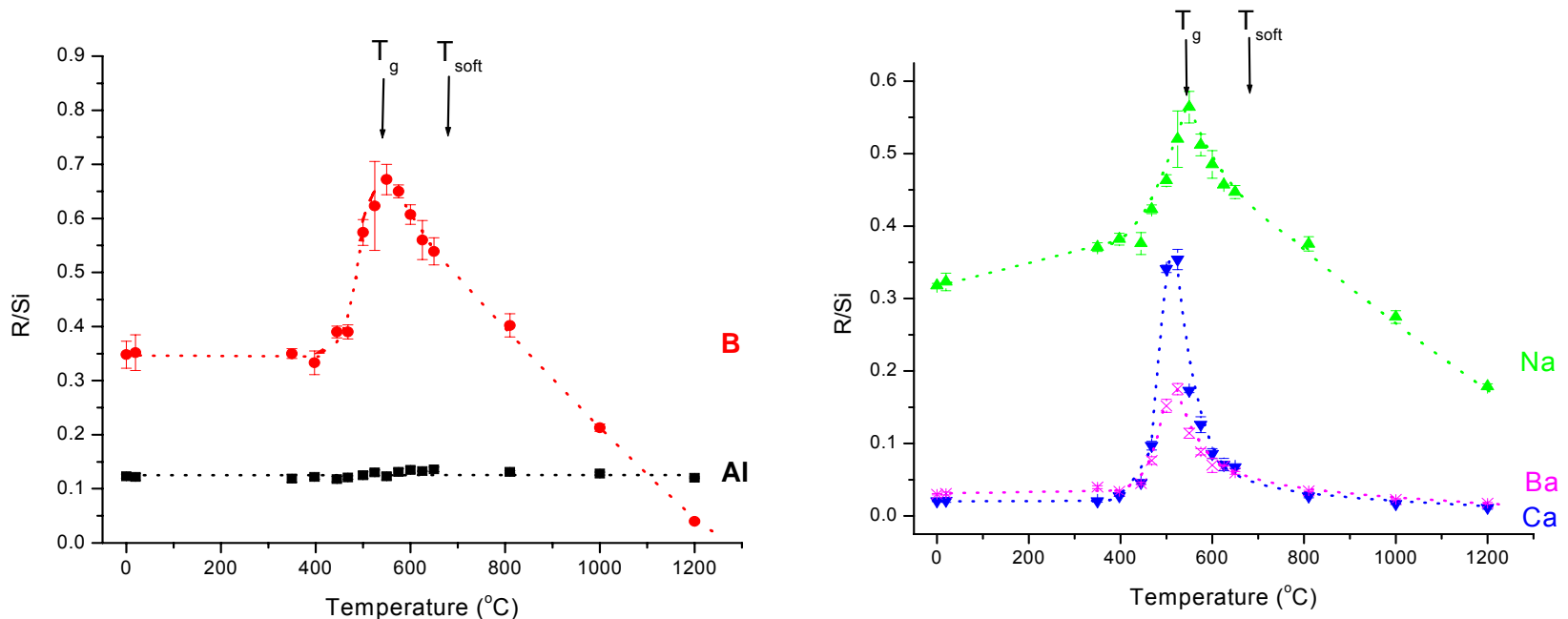
**EELS (and XPS)
confirm that this
surface layer is
depleted in boron.**



The thickness of the surface layer is NOT related to the fiber diameter (FA)



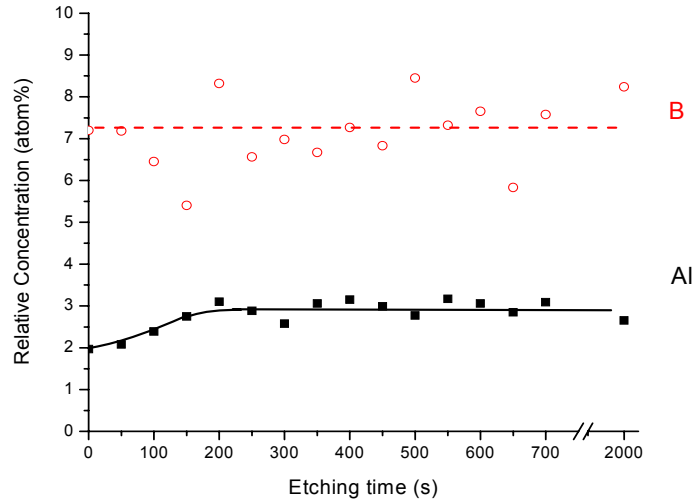
'Isothermally' Freezing in the Surface Composition



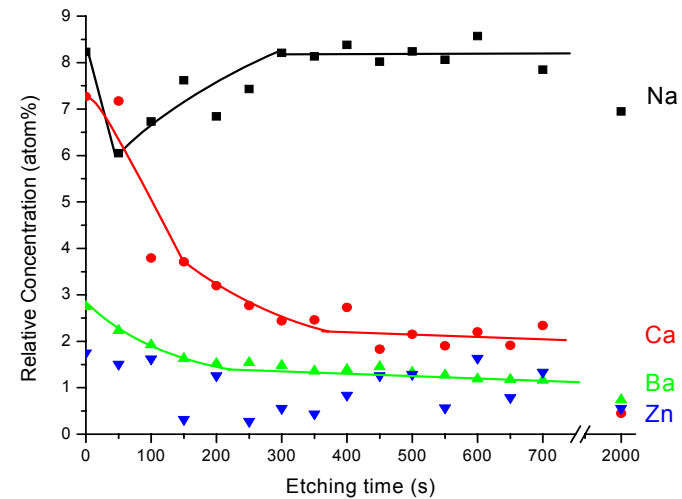
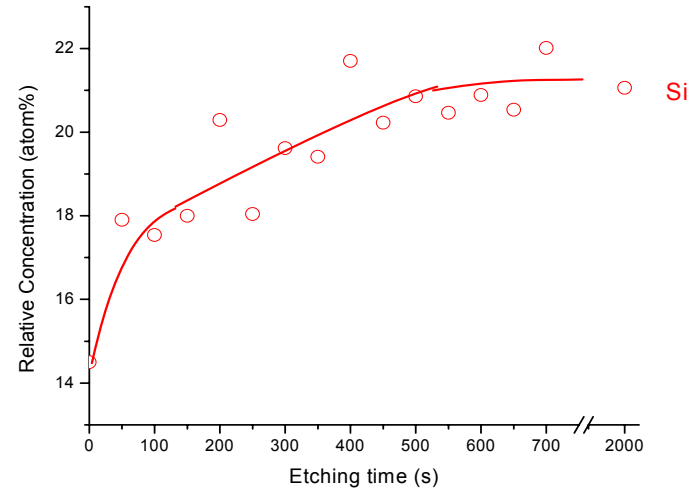
- after heat-treatment at T_g , the surface is depleted in Si. The concentrations of B, Na, Ba and Ca increase significantly on the surface, especially Ca and Ba.
- At temperatures > 800 °C, the surface is depleted in B and Na.
- The Al/Si ratio does not change over the entire temperature range.

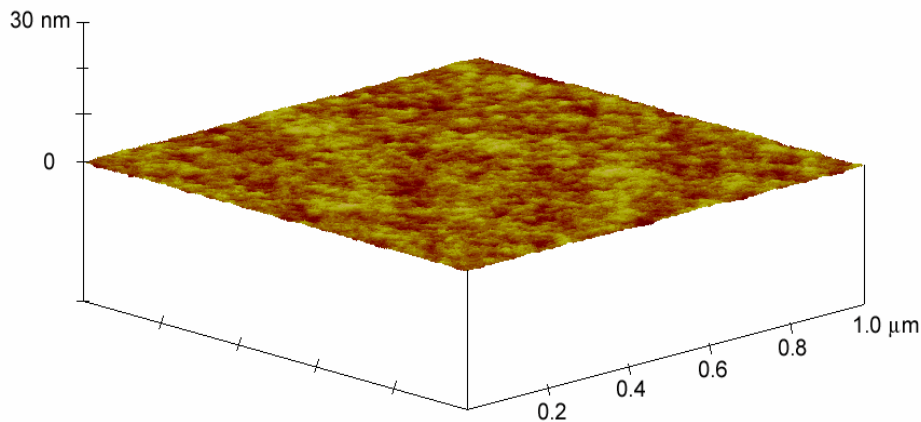
Glass VII

XPS Depth Profiling:
air-fracture surface of glass I,
“equilibrated” at 525 °C.

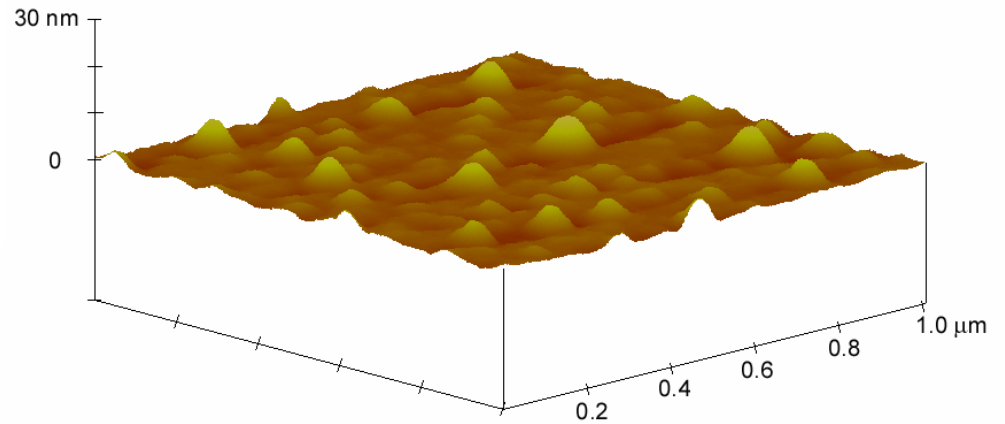


- Sputtering rate $\sim 1 \text{ \AA/s}$.
- The Si-depleted layer $\sim 200 \text{ \AA}$ thick.






Before: RMS = 0.14 nm



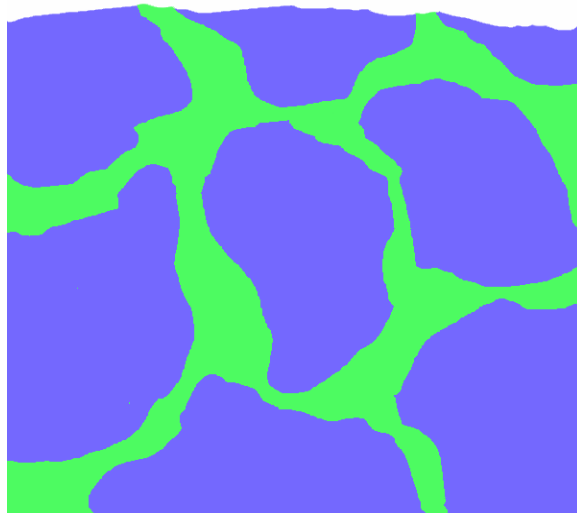
After: RMS = 0.93 nm

After heat-treatment, features (4-7 nm in height) appear on the surface.

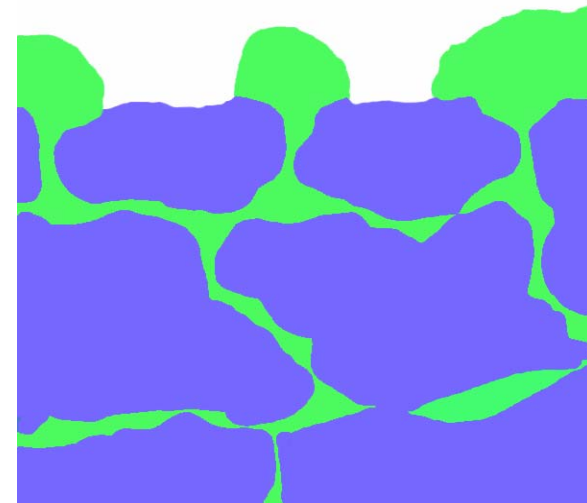
Phenomenological Model for “Phase Segregation/Migration” to the Surface

 Network modifier rich region

 Network former rich region



Before Heat-treatment



After Heat-treatment

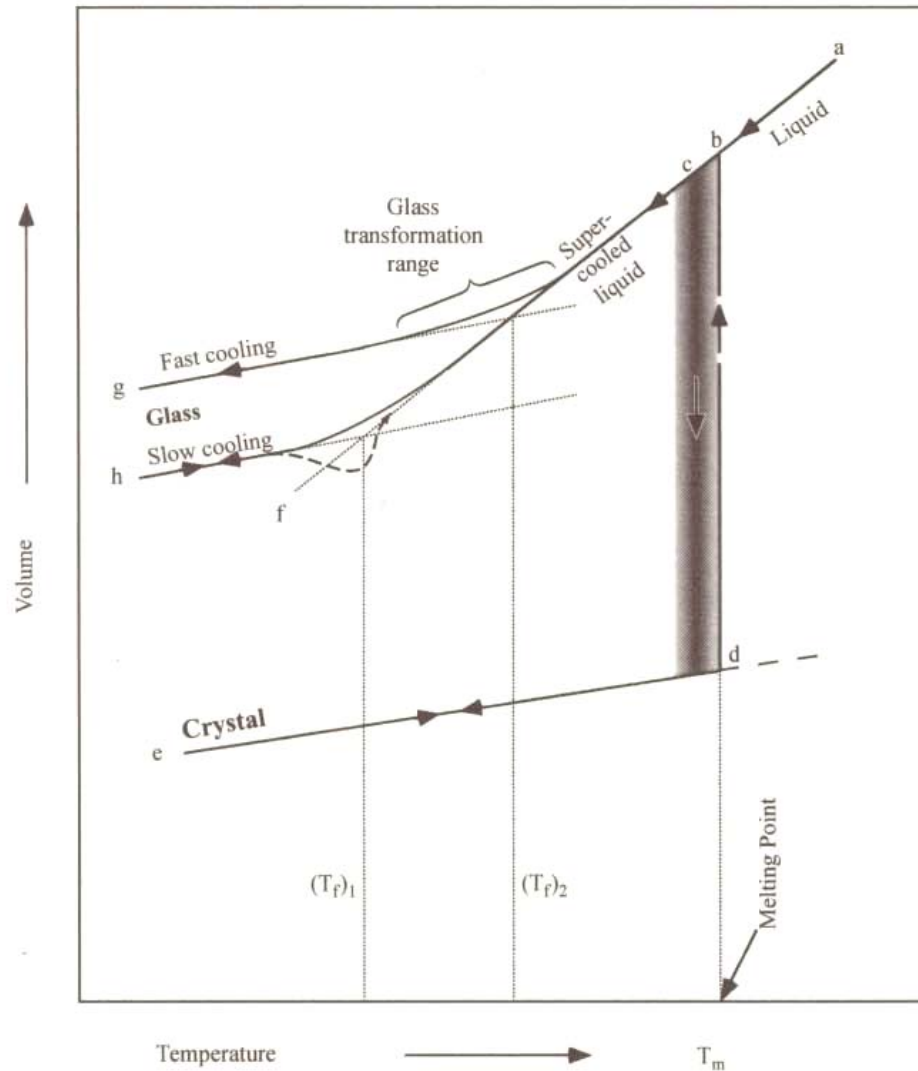
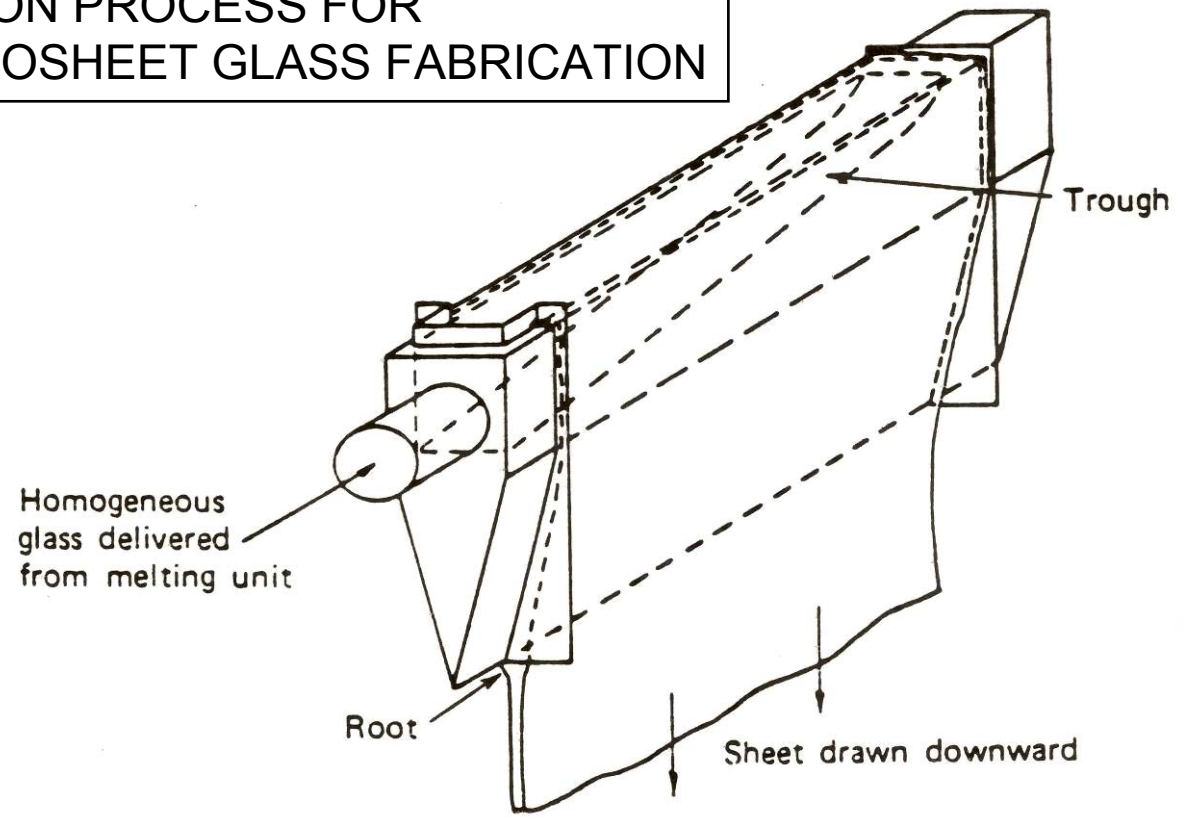


FIGURE 5.1 The volume-temperature diagram. (After A. K. Varshneya, *Fundamentals of Inorganic Glasses*, Fig. 2-1, p. 15, Academic Press, 1994.)

FUSION PROCESS FOR
MICROSHEET GLASS FABRICATION



5X surface segregation
of Sb (.5% in the bulk for fining)

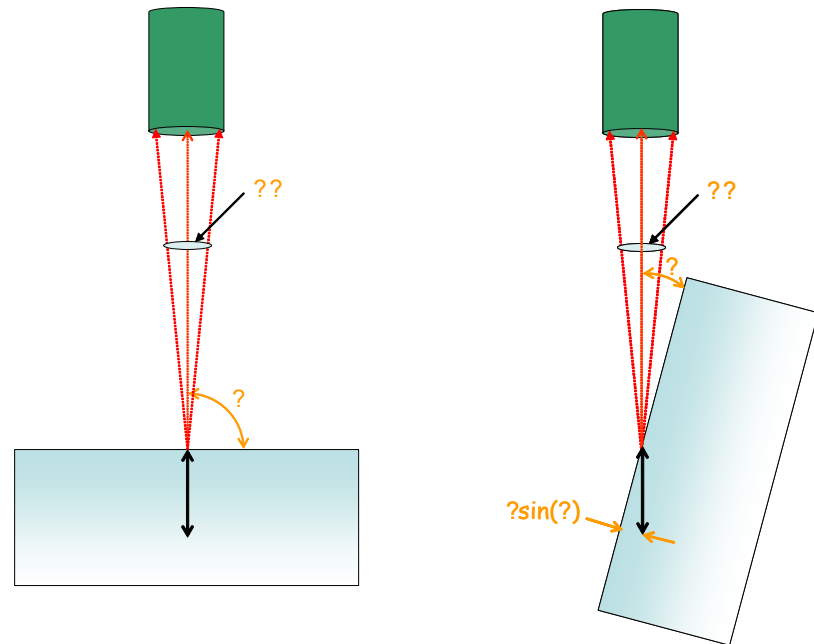
Angle Resolved XPS Depth Profiling

Beer-Lambert Law
$$I = I_0 e^{-z / \lambda \sin \theta}$$

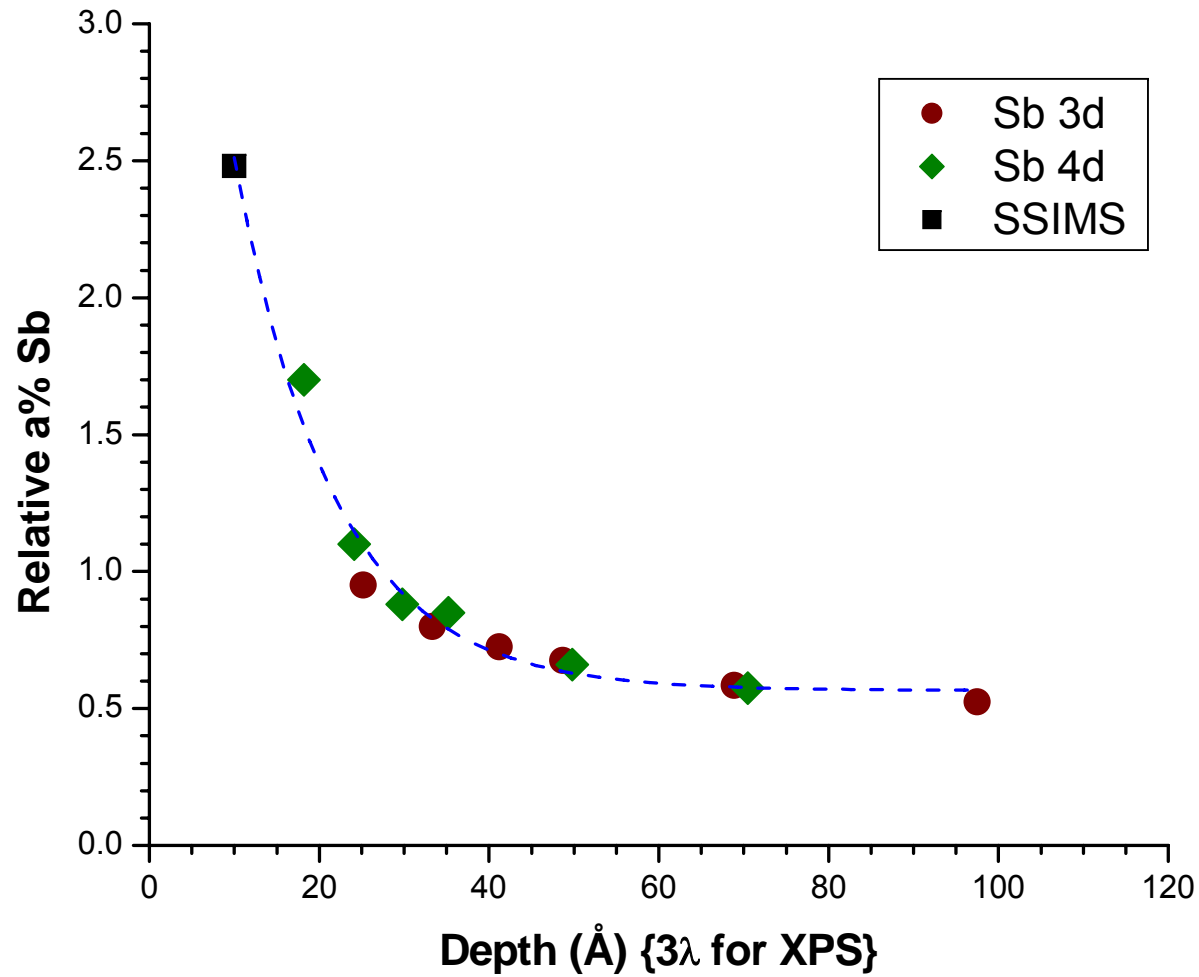
Observed intensity, I , as a function of depth, z where λ is escape depth, θ is takeoff angle (w.r.t. surface plane).

Case 1. Atomically clean surface;
no angular effect

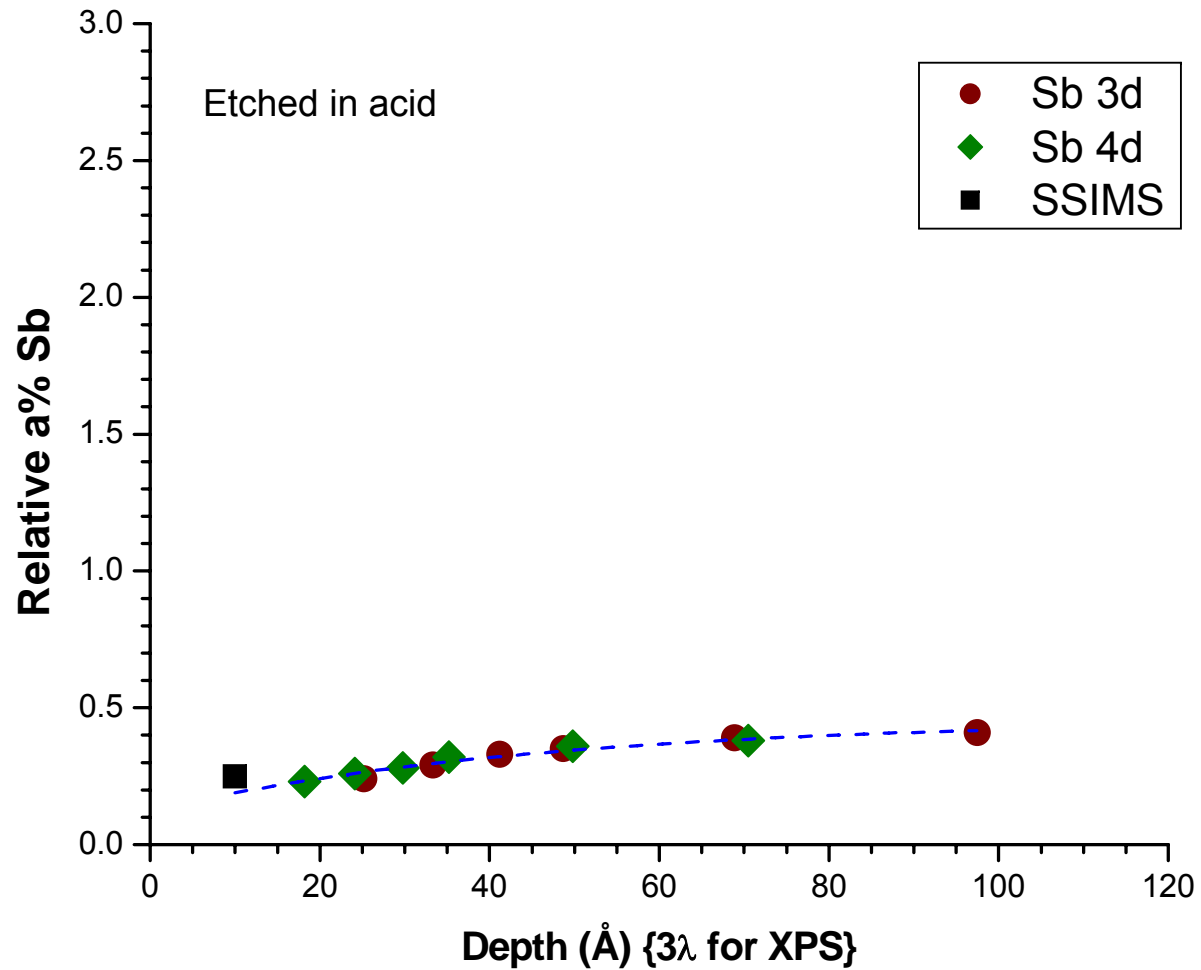
Angle Resolved Depth Profiling in XPS



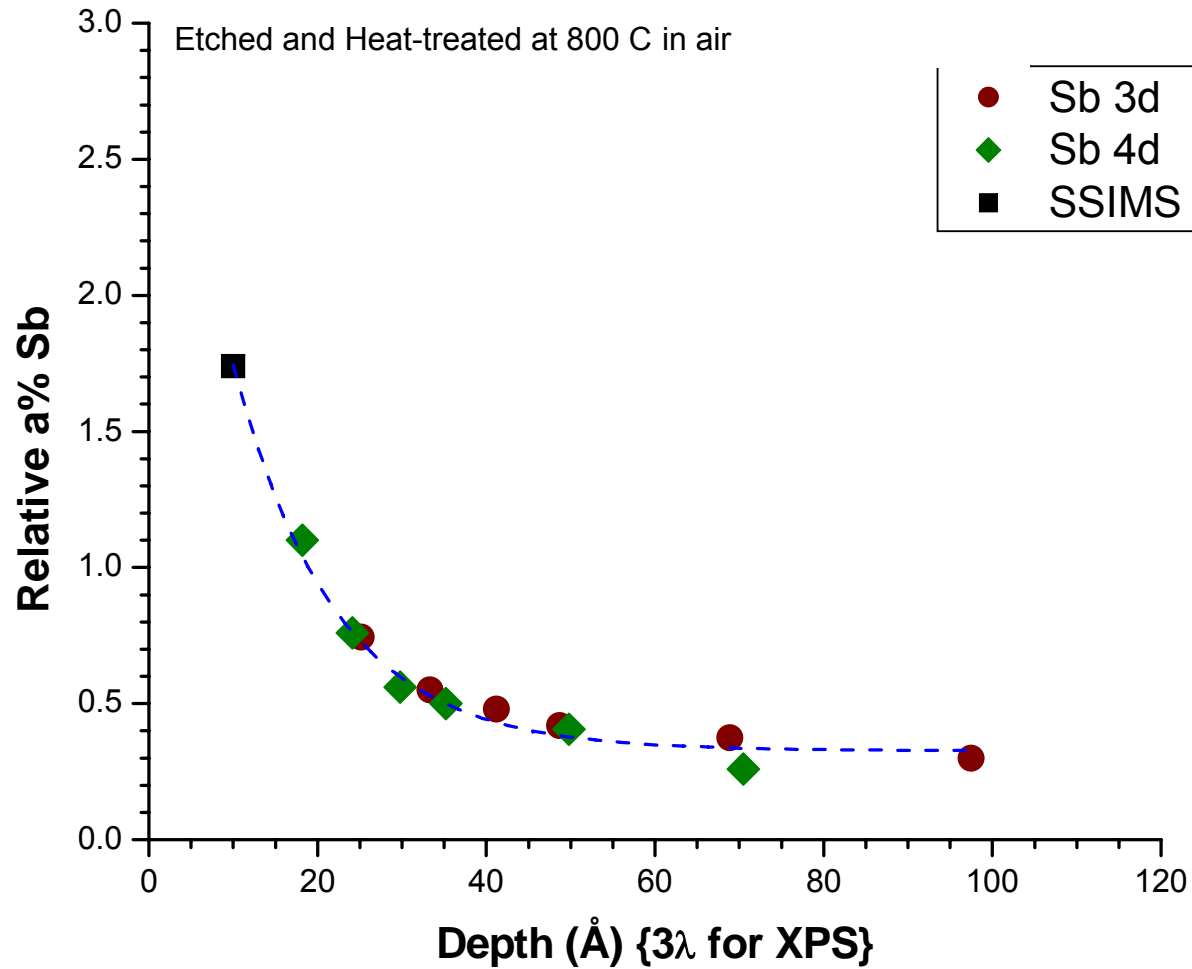
Antimony Depth Distribution by Angle-Resolved XPS and FAB-Static SIMS



Antimony Depth Distribution by Angle-Resolved XPS and FAB-Static SIMS

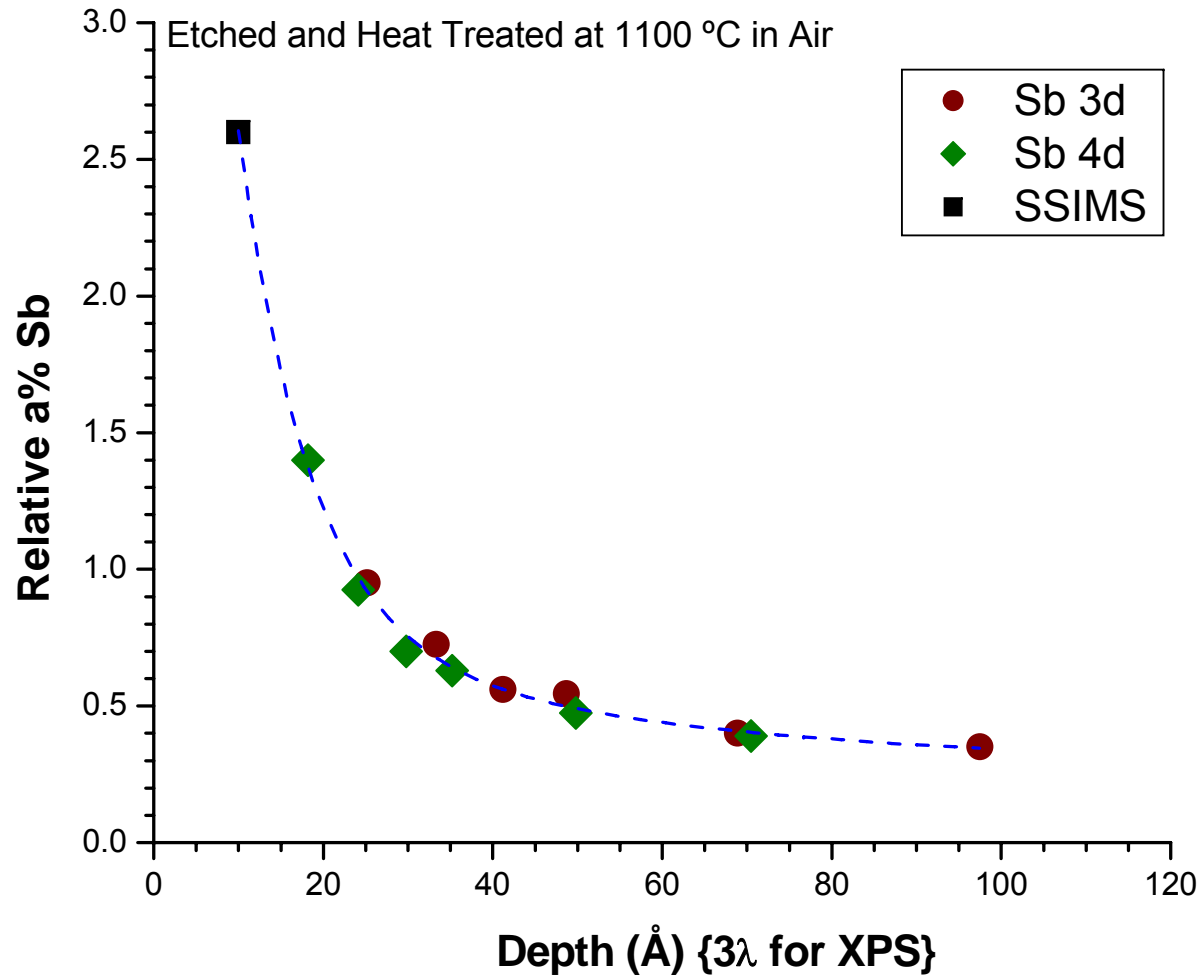


Antimony Depth Distribution by Angle-Resolved XPS and FAB-Static SIMS



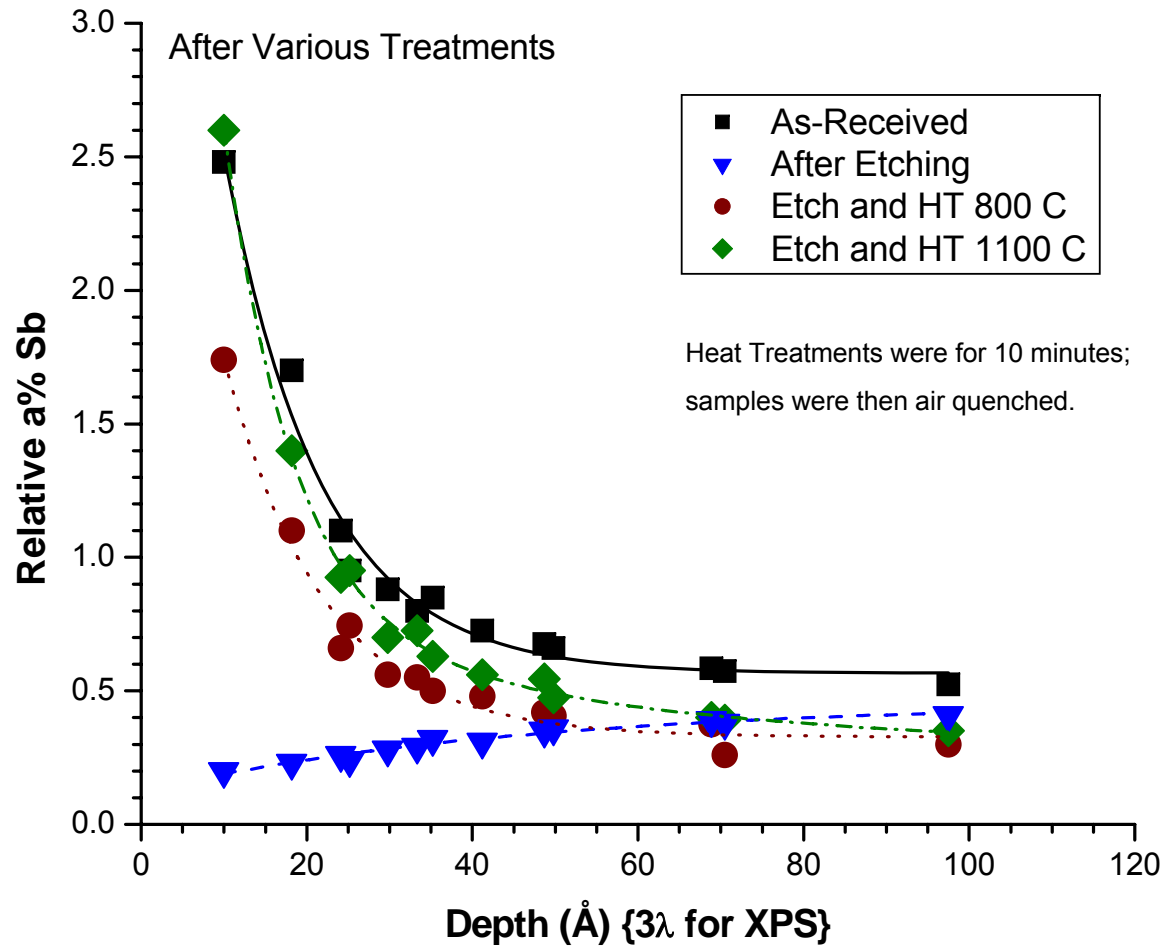
*Heat Treatments were for 10 minutes; samples were then air quenched.

Antimony Depth Distribution by Angle-Resolved XPS and FAB-Static SIMS



*Heat Treatments were for 10 minutes; samples were then air quenched.

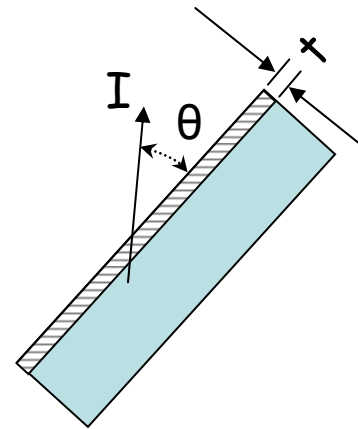
Antimony Depth Distribution by Angle-Resolved XPS and FAB-Static SIMS



Case 2. Thin, uniform layer A of thickness, t , on top of substrate B
(where $E_{k,A} = E_{k,B}$)

$$I_A = I_A^\infty \left[1 - \exp\left(-t/\lambda_A \sin \theta\right) \right]$$

$$I_B = I_B^\infty \exp\left(-t/\lambda_B \sin \theta\right)$$

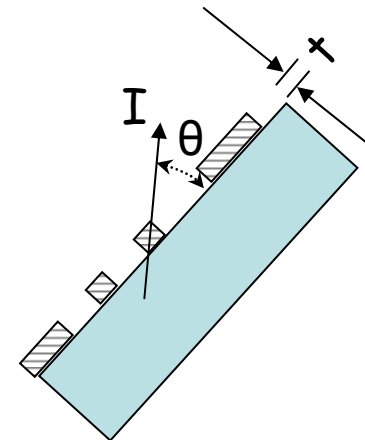


Ratio,

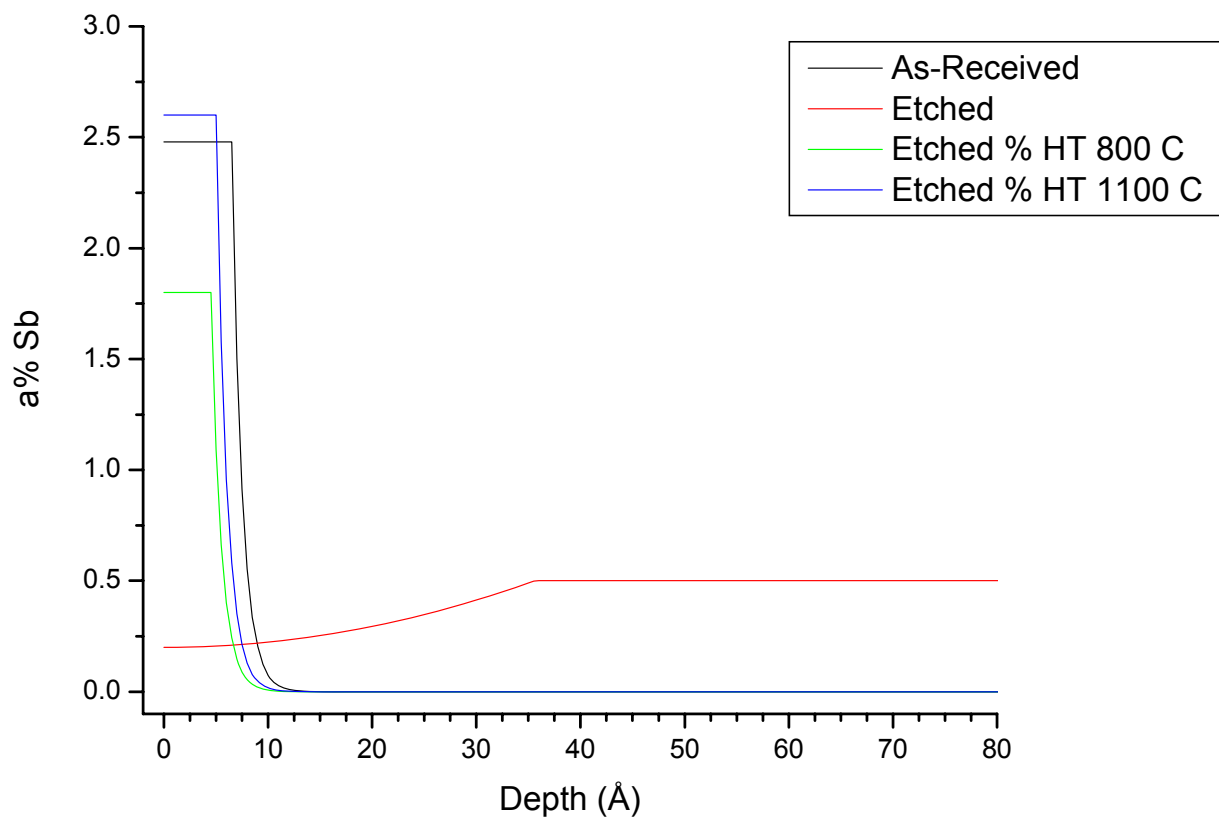
$$\frac{I_A}{I_B} = \frac{I_A^\infty \left(1 - \exp^{-t/\lambda_A \sin \theta} \right)}{I_B^\infty \left(\exp^{-t/\lambda_B \sin \theta} \right)}$$

Case 3. Thin, patched layer A of thickness, t , on top of substrate B where γ is the fractional coverage of A

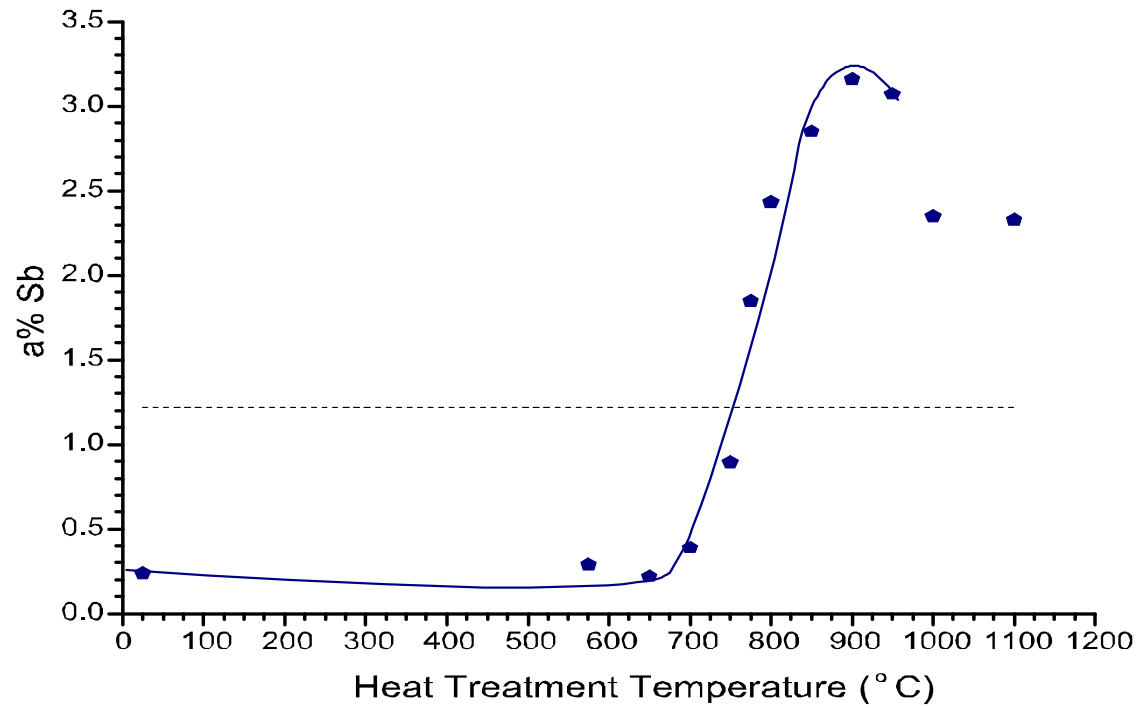
$$\frac{I_A}{I_B} = \frac{I_A^\infty}{I_B^\infty} \left[\frac{\gamma(1 - \exp^{-t/\lambda_A \sin \theta})}{(1 - \gamma) + \gamma(\exp^{-t/\lambda_B \sin \theta})} \right]$$



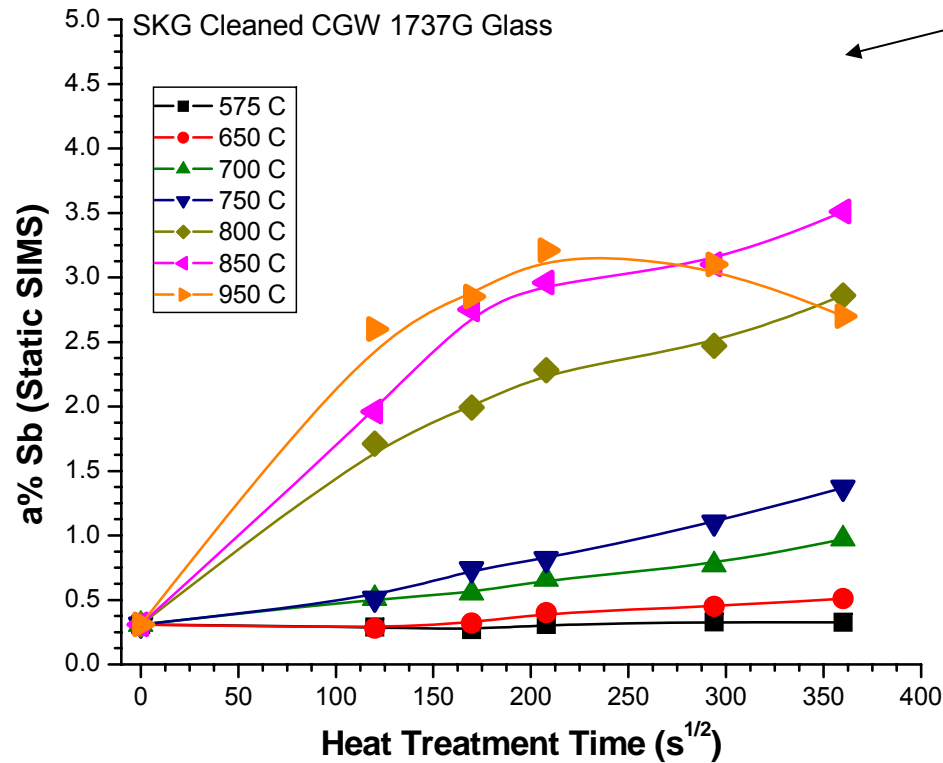
Reconstructed Angle Resolved XPS Depth Profiles



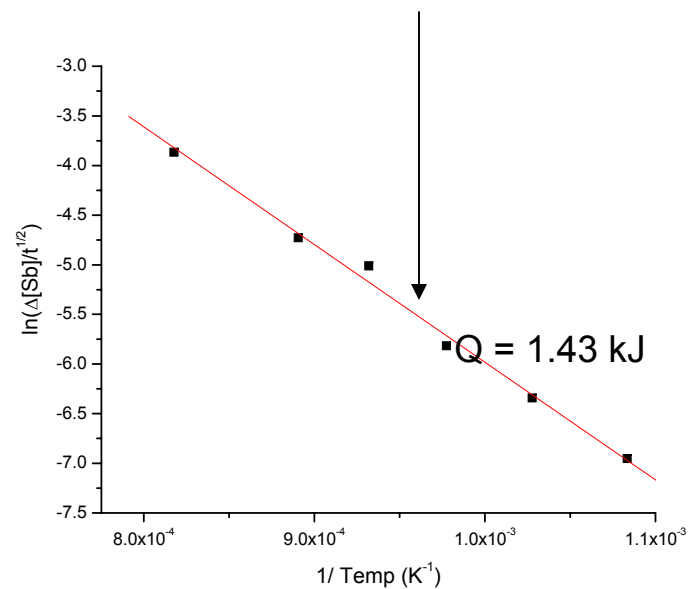
FAB-Static SIMS Analysis of Sb segregation versus temperature



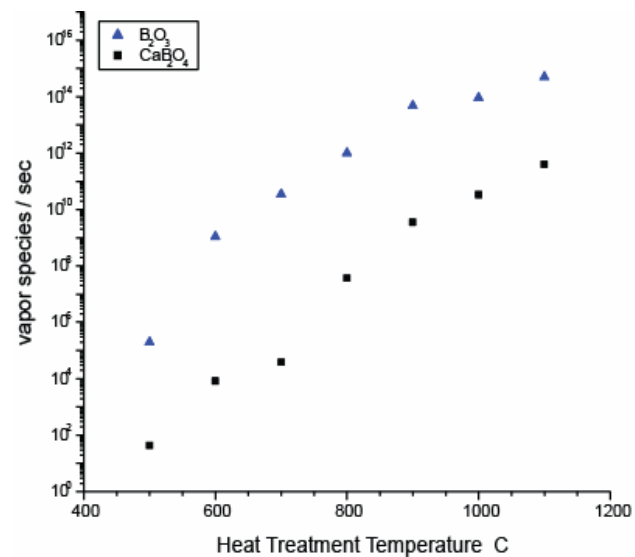
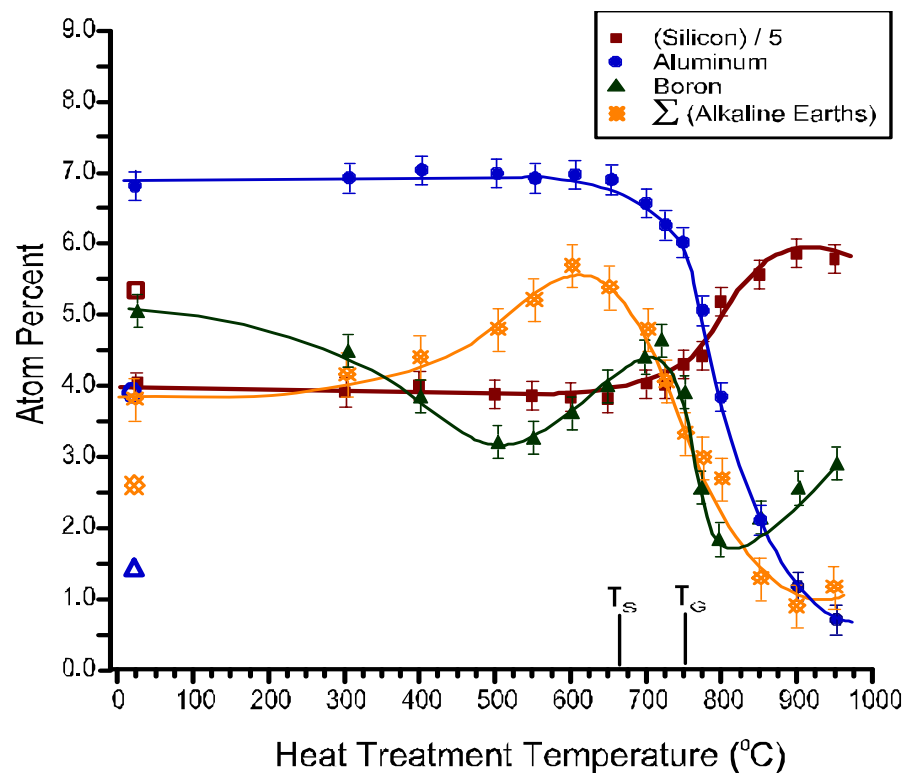
Surface Concentration of Antimony on Etched and Heat Treated Glass by Static SIMS



The graph on the left suggests that the enrichment of Sb occurs through bulk diffusion. Using only the linear portions of this concentration graph on the left, the activation energy for Sb diffusion is calculated below.



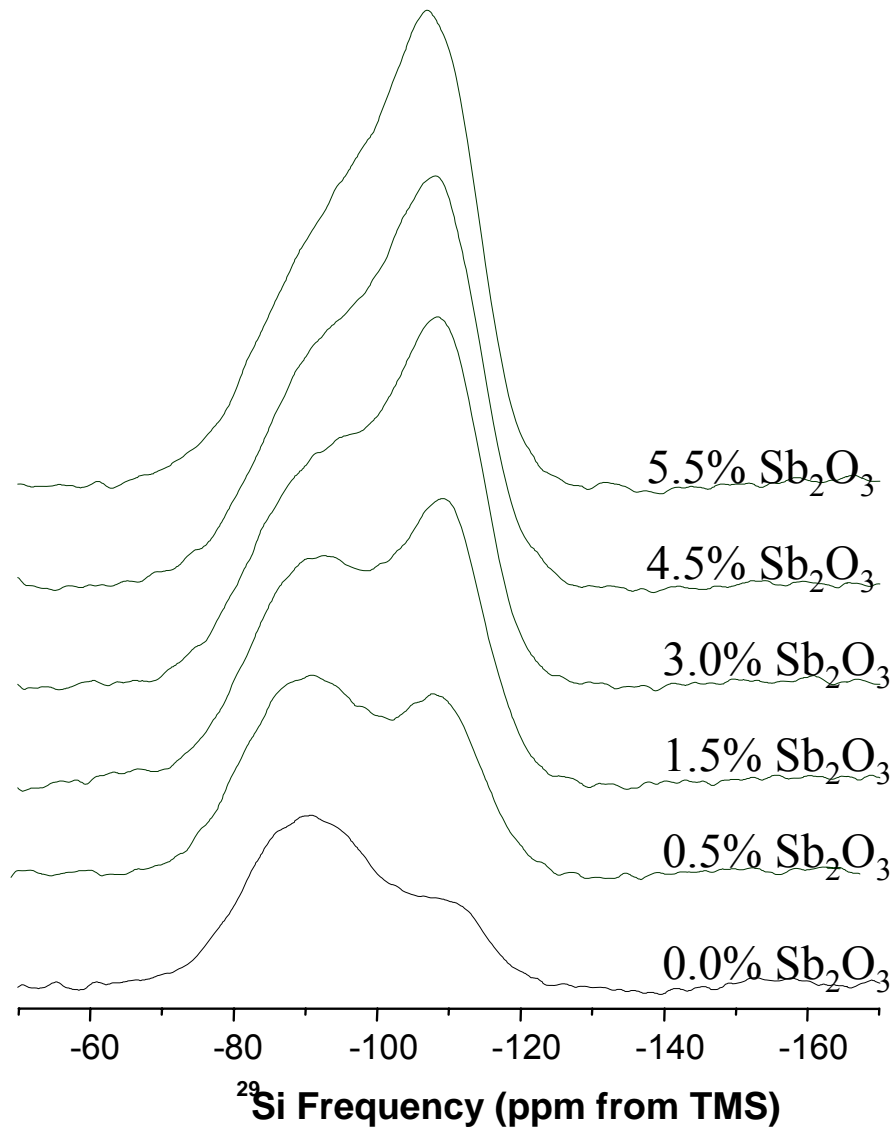
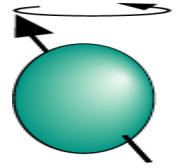
surface composition by FAB SIMS for commercial microsheet glass for FPD



Estimated 'Initial' Molecular Flux of Boron Containing Vapor Species from CGW 1737 Fracture Surface.



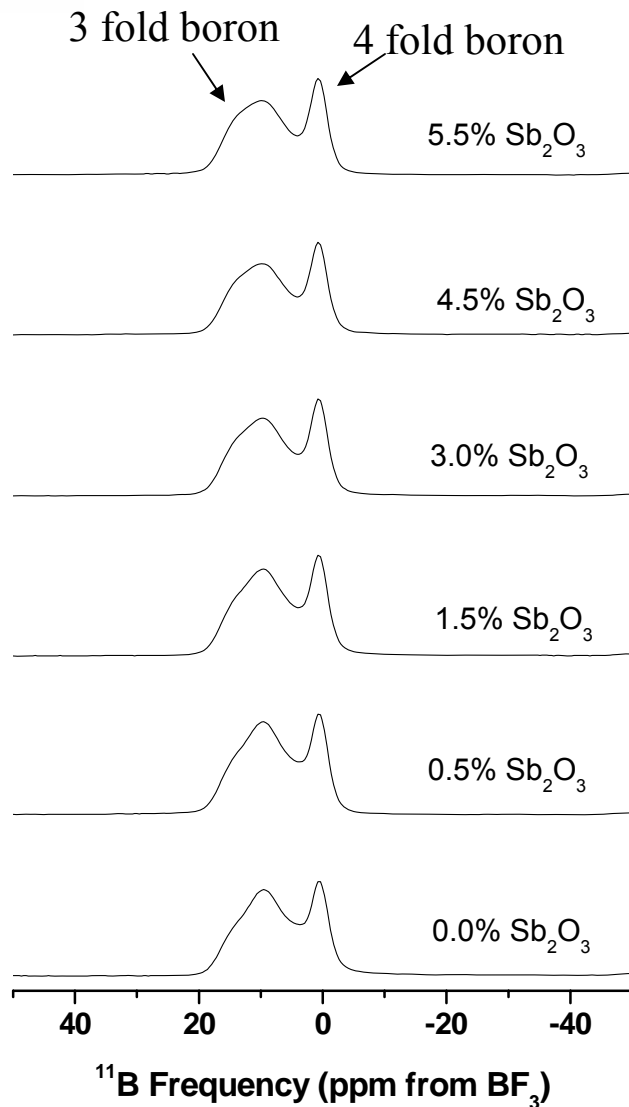
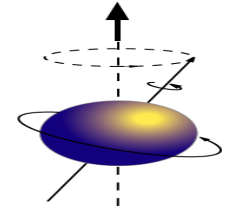
^{29}Si MAS NMR



More $\text{Q}^4(4\text{Si})$ units are observed as the antimony oxide concentration increases.



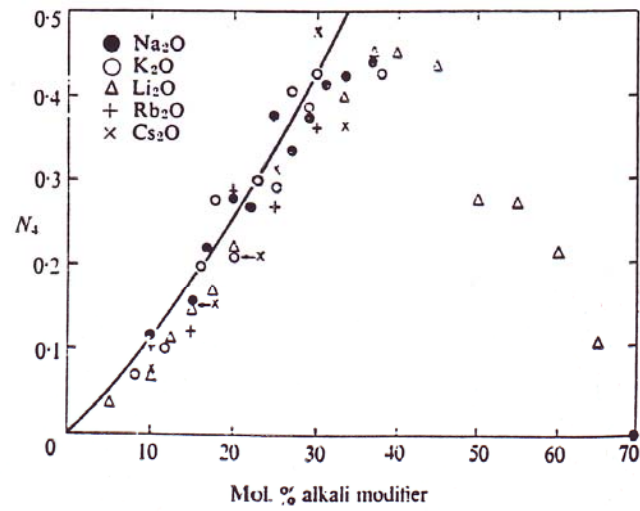
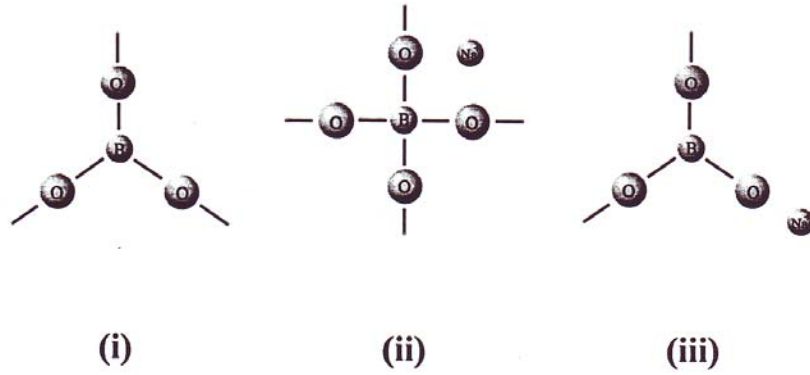
^{11}B MAS NMR



% Sb_2O_3	Ratio of 4/3 Fold Boron
0.0	0.45
0.5	0.50
1.5	0.57
3.0	0.66
4.5	0.62
5.5	0.66

With an increase in Sb_2O_3 concentration, there is an increase in tetrahedral boron units.

Boron-oxide in glass



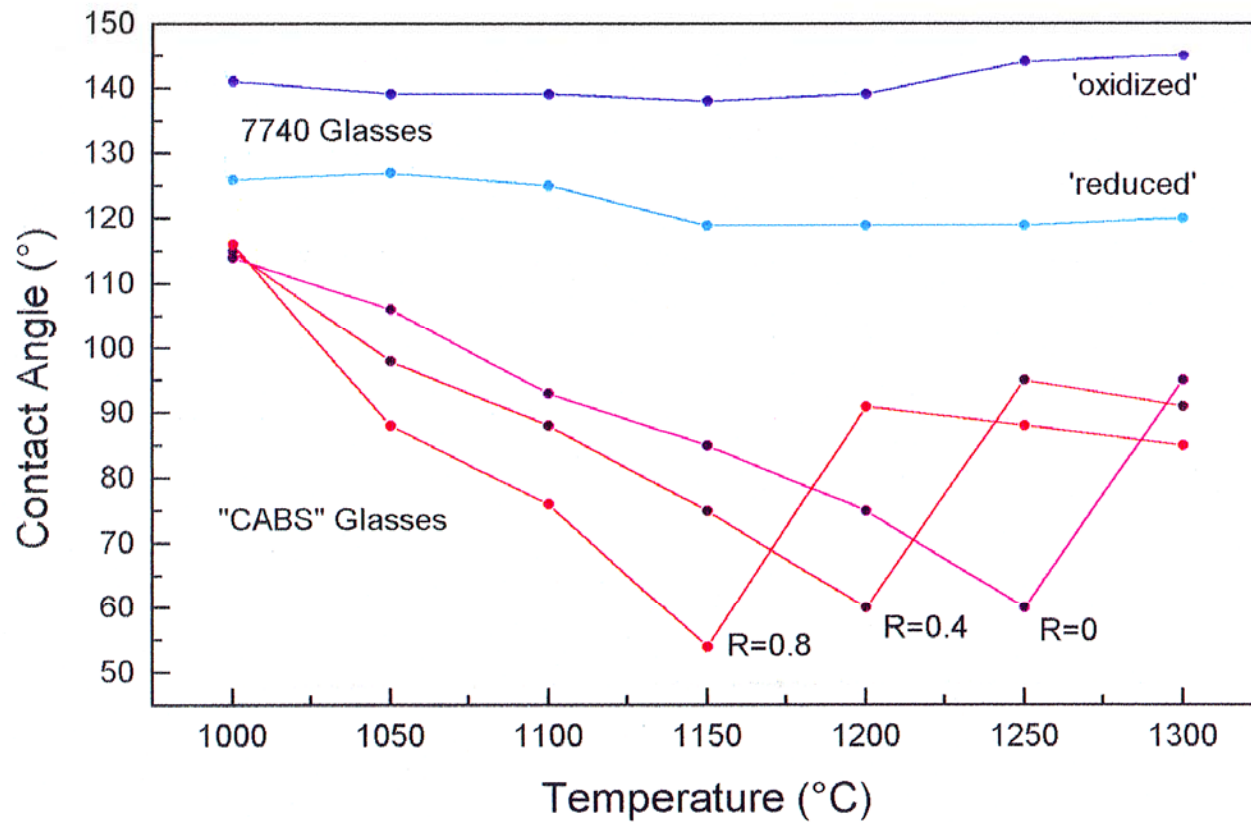
$$R = \frac{x R_2O}{(1-x) B_2O_3}$$

Surface Tension of Borate Glasses

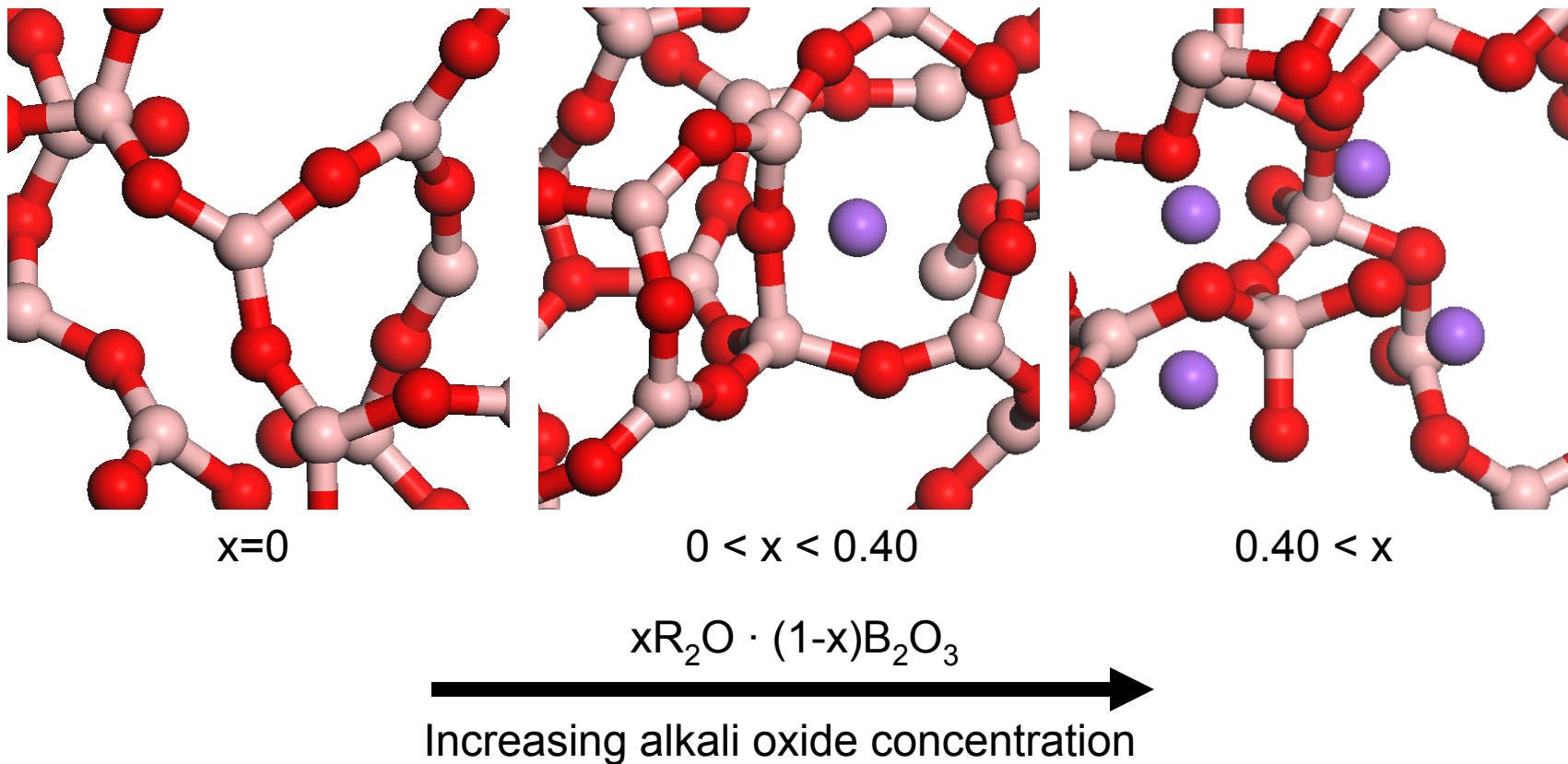
- $B_2O_3 \sim 80$ dyn/cm at $1000^\circ C$
- positive temperature coefficient
- exhibits boron oxide anomaly
- temperature coefficient is constant up to 20m/o R_2O

Altogether, these data suggest the segregation and orientation of planar $[BO_3]$ at the surface.

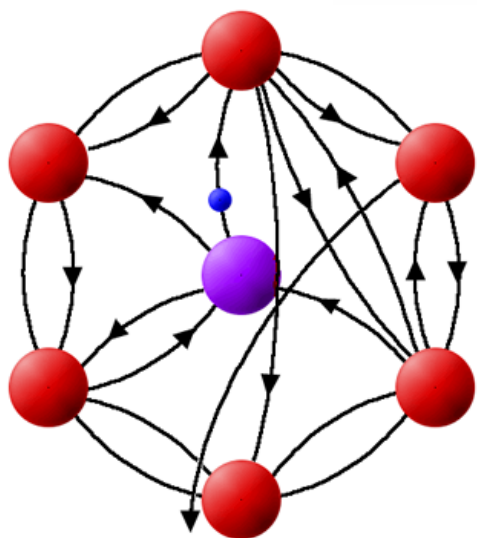
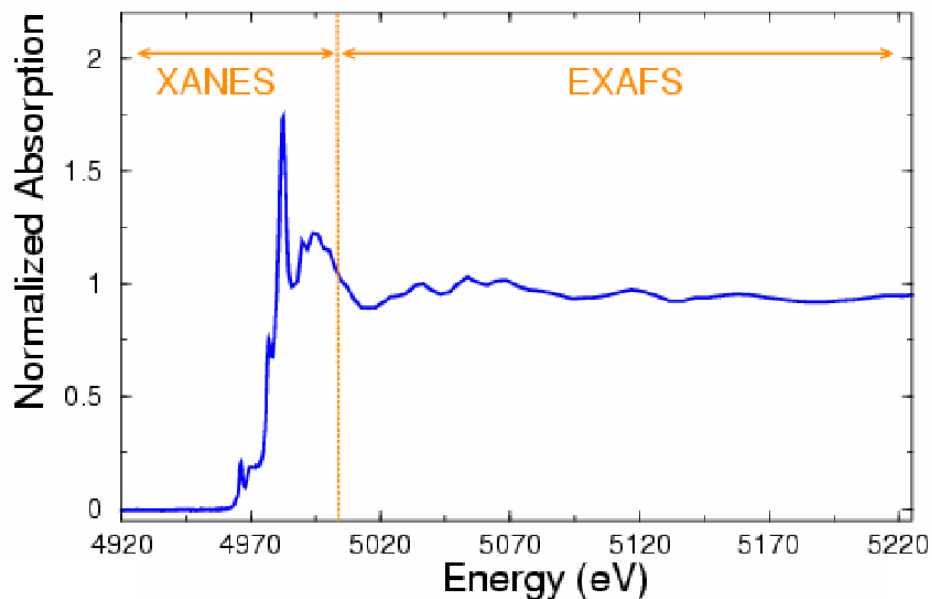
Contact Angles of Borosilicate Glasses on Silicon Carbide



Boron in the bulk and at surfaces:

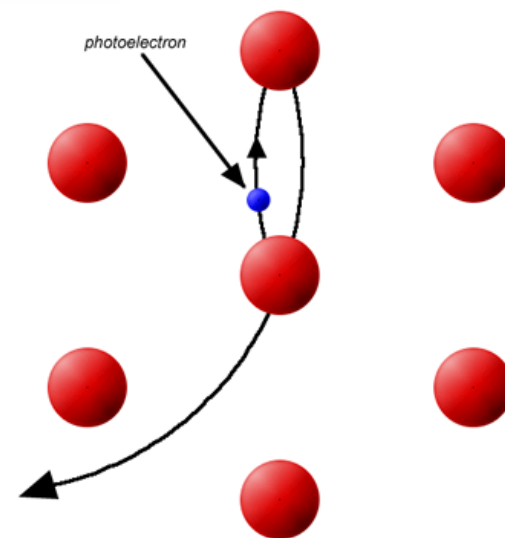


XANES vs. EXAFS

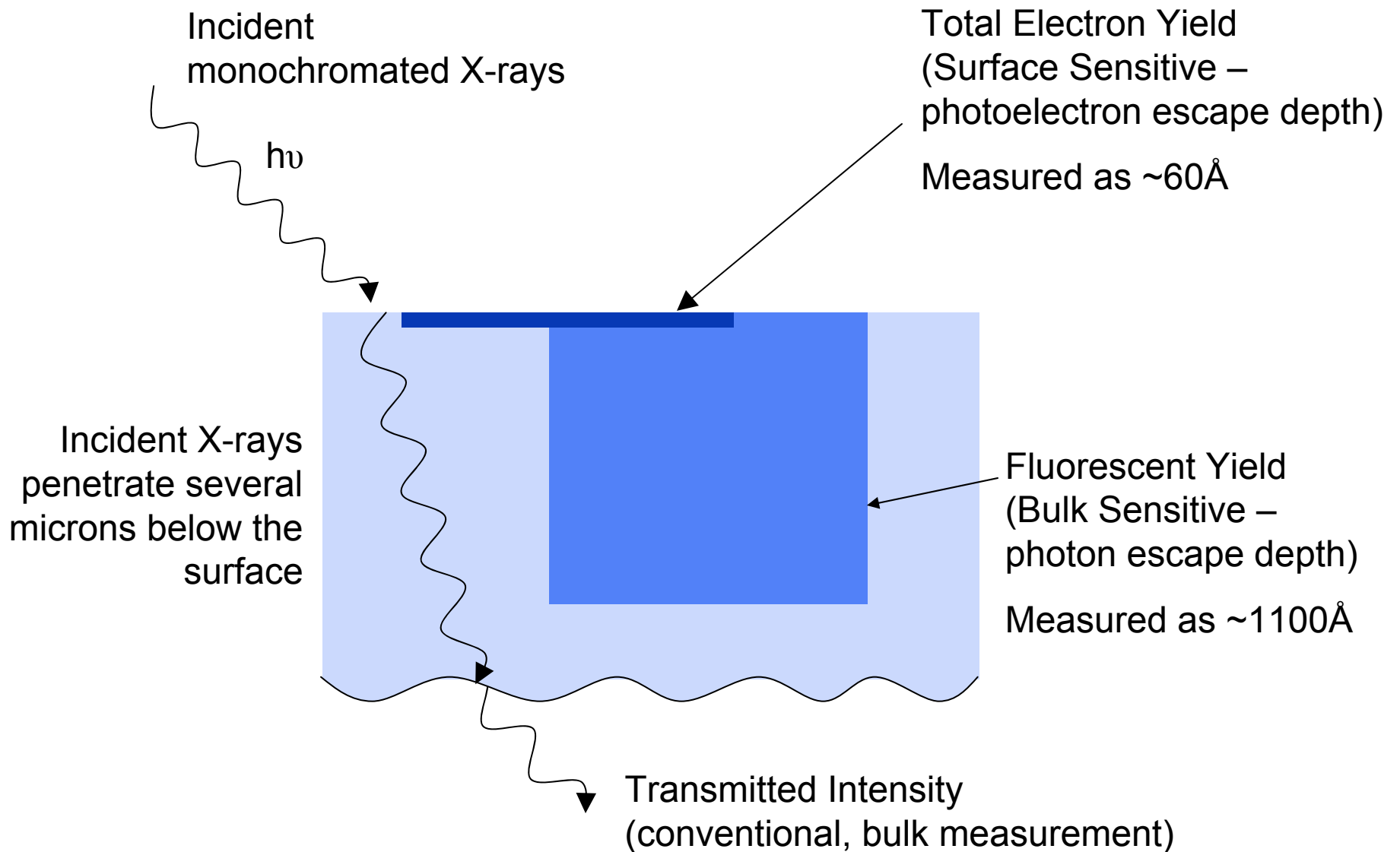


XANES is dominated by multiple scattering processes of low kinetic-energy photoelectrons.

EXAFS contains oscillations from scattering by high kinetic energy photoelectrons.



Surface Sensitivity



Boron XANES at mineral surfaces

Peak A: only 3-fold boron

Peak B: only 4-fold boron

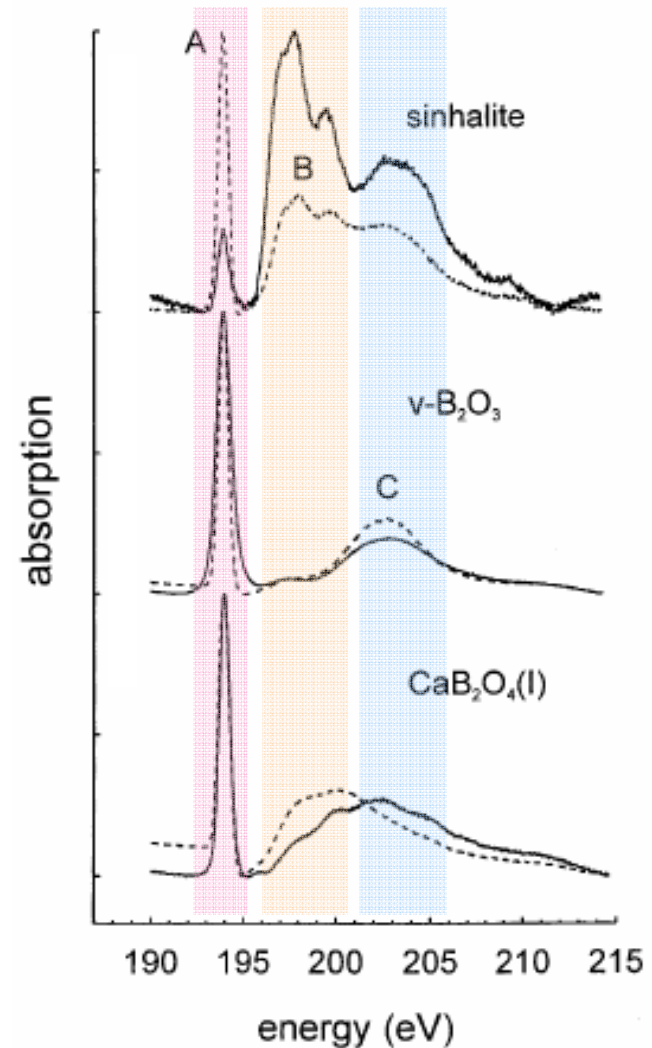
Peak C: contains information from both
3- and 4-fold boron

Solid spectra:

FY – bulk measurement

Broken spectra:

TEY – surface measurement



* Figures borrowed from Fleet and Lui, Phys. Chem. Minerals (2001).

SUMMARY:

opportunities for glass surface modification

- controlled electrical conductivity
- 'primed' for adhesion
- 'hardened' for abrasion resistance
- anti-reflective or highly reflective
- soluble or insoluble